CHEMISTRY
A EUROPEAN JOURNAL

DOI: 10.1002/chem.200601699

Catalyzing Aldehyde Hydrosilylation with a Molybdenum(VI) Complex: A Density Functional Theory Study

Paulo Jorge Costa,[a] Carlos C. Romão,[b] Ana C. Fernandes,[b] Beatriz Royo,[b] Patrícia M. Reis,[b] and Maria José Calhorda*[a]

Abstract: $[MoCl_2O_2]$ catalyzes the hydrosilylation reaction of aldehydes and ketones, as well as the reduction of other related groups, in apparent contrast to its known behavior as an oxidation catalyst. In this work, the mechanism of this reaction is studied by means of density functional theory calculations using the B3LYP functional complemented by experimental data. We found that the most favorable pathway to the first step, the Si–H activation, is a [2+2] addition to the Mo=O bond, in agreement with previous and related work. The stable intermediate that results is a distorted-square-pyramidal hydride complex. In the following step, the aldehyde approaches this species and coordinates weakly through the oxygen atom. Two alternative pathways can be envisaged: the classical reduction, in which a hydrogen atom migrates to the carbon atom to form an alkoxide, which then proceeds to generate the final silyl ether, or a concerted mechanism involving migration of a hydrogen atom to a carbon atom and of a silyl group to an oxygen atom to generate the silyl ether weakly bound to the molybdenum atom. In this Mo^{VI} system, the gas-phase free energies of activation for both approaches are very similar, but if solvent effects are taken into account and $HSiMe_3$ is used as a source of silicon, the classical mechanism is favored. Several unexpected results led us to search for still another route, namely a radical path. The energy involved in this and the classical pathway are similar, which suggests that hydrosilylation of aldehydes and ketones catalyzed by $[MoCl_2O_2]$ in acetonitrile may follow a radical pathway, in agreement with experimental results.

Keywords: CO reduction · density functional calculations · hydrosilylation · molybdenum · radical reactions

Introduction

The chemistry of molecular oxo complexes of Groups 6 and 7 began to take shape through the quest for molecular olefin metathesis catalysts,[1] and became synthetically refined after the discoveries of $[ReCp^*O_3]$[2] and $[ReMeO_3]$[3] disclosed a bright palette of new catalysts and reaction models for oxidative and oxygen-transfer reactions.[4] Therefore, it was with great surprise[5] that one such complex, namely, $[ReIO_2(PPh_3)_2]$, was found to also catalyze reductive reactions such as the hydrosilylation of aldehydes and ketones, as reported by Toste and co-workers.[6] Before this, the highly developed carbonyl hydrosilylation reaction had remained an area ruled by low-oxidation-state transition-metal catalysts.[7] This reductive activity of oxo complexes is perhaps not so surprising, at least in nature, when one considers that the reactions carried out by enzymes containing, for instance, the $[MoO_2]^{2+}$ active center, are reversible, and operate in both oxidative and reductive modes. The most obvious example is given by the aldehyde oxidoreductase enzymes in which $[MoO_2]^{2+}$ centers may catalyze oxidation to carboxylic acids, as well as aldehyde reduction to alcohols.[8]

This led us to study the reductive activity of the simplest molybdenyl derivative, $[MoCl_2O_2]$, which proved to be an active catalyst for the hydrosilylation of aldehydes and ketones.[9] Further studies by some of us, as well as by Abu-Omar's group, showed that these reactions can be catalyzed by a wide range of molecular oxo complexes of Re and Mo, including the $[ReO_3]^+$, $[ReO_2]^+$, $[ReO]^{3+}$, $[MoO_2]^{2+}$, and $[MoO]^{3+}$ metal cores with a variety of classical and organometallic ligands.[10,11]

[a] P. J. Costa, Prof. M. J. Calhorda
Departamento de Química e Bioquímica
Faculdade de Ciências, Universidade de Lisboa
1749-016 Lisboa (Portugal)
Fax: (+351) 217-500-088
E-mail: mjc@fc.ul.pt

[b] Prof. C. C. Romão, Dr. A. C. Fernandes, Dr. B. Royo, P. M. Reis
Instituto de Tecnologia Química e Biológica
Av. da República, EAN, Apart. 127, 2781-901 Oeiras (Portugal)

To date, the most active catalysts reported have been cationic $[Re(hoz)_2O]^+$[11] (hoz: 2-(2′-hydroxyphenyl)oxazoline(−)) and Re_2O_7[10] in the case of Re, and $[MoCl_2O_2]$ in the case of Mo.[12] In the latter, replacement of Cl by other alkyl, aryl, cyclopentadienyl, O, or S ligands clearly diminishes the catalytic activity and thus requires higher temperatures for the reaction to occur. Interestingly, the only totally unreactive species found in our studies up to now is the dithiocarbamate complex $[MoO_2(S_2CNEt_2)_2]$, which, considering the nature of its ligands, is closest to the enzymatic molybdenyl active centers.[12] In the case of Re–dioxo species, $[ReCl_3(dppe)O]$ (dppe: 1,2-bis(diphenylphosphanoethane) is also unreactive.[13]

The synthetic value of these hydrosilylation reactions combines high activities with cheap, readily available catalysts as well as compatibility with a large variety of functionalities on the carbonyl compounds. Besides aldehydes and ketones, these reductive processes have been extended to the reduction of imines,[14] esters,[15] sulfoxides (to thioethers), and pyridine-*N*-oxides (to pyridines) catalyzed by $[MoCl_2O_2]$.[16] Oxazoline derivatives of $[ReO]^{3+}$ led to an enantioselective imine reduction with enantiomeric excess (*ee*) values in the range of $>98\,\%$.[13]

The hydrosilylation reaction of organic carbonyls implies that Si–H bond activation occurs because it involves the transfer of the H atom in R_3SiH to the carbonyl carbon atom of R_2CO or RHCO. In his seminal study, Toste showed the presence of a Re–H intermediate species by using ^1H NMR spectroscopy, which led him to propose the mechanism depicted in Scheme 1.[6]

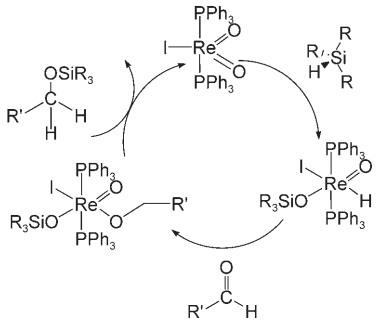

Scheme 1.

In the first step, the Si–H bond adds across one Re=O bond in a [2+2] fashion. Another alternative to form the same hydride would be the [3+2] addition, leading to a mixed $[ReI(HO)(OSiMe_3)(PPh_3)_2]$ species, which possibly tautomerizes fast to $[ReI(H)(O)(OSiMe_3)(PPh_3)_2]$, as proposed by Thiel.[5]

In the case of the cationic monooxo complex catalyst $[Re(hoz)_2O]^+$, Abu-Omar and co-workers ruled out the participation of a hydride intermediate in the mechanism on the basis of results obtained from isotopic labeling and kinetic experiments.[11] These results included the confirmation of the low hydricity of the corresponding hydride $[ReH(hoz)_2(O)]$, which does not react with aldehydes. As an alternative, a σ-bond metathesis-type mechanism was proposed as depicted in Scheme 2. This mechanism is consistent with the observed kinetic isotope effects ($Et_3SiH/Et_3SiD = 1.3$).

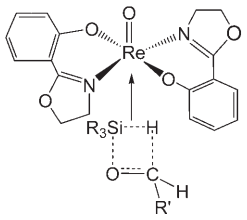

Scheme 2.

In a very recent publication, Wu, Lin, and co-workers reported a thorough density functional theory (DFT) study of the hydrosilylation of acetaldehyde with Me_3SiH catalyzed by $[ReI(O)_2(PR_3)_2]$ (R = Me, Ph).[17] Their results suggested that the most favorable pathway starts with PR_3 dissociation, followed by [2+2] addition of Si–H to the Re=O bond, coordination of the aldehyde to the Re atom, reduction of the coordinated aldehyde to alkoxide, rearrangement, and a final intramolecular attack of the alkoxide on the Si atom of the coordinated siloxide, as depicted in Scheme 3.

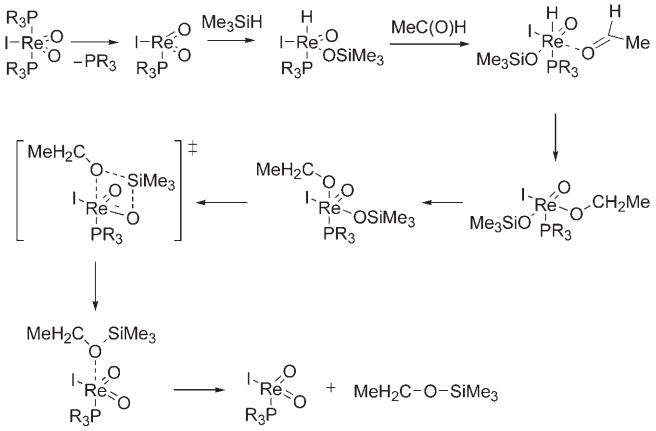

Scheme 3.

The [2+3] addition, as well as the σ-bond metathesis alternatives, were not supported by the computational results, which also addressed several other mechanistic possibilities.

In our studies with the $[MoCl_2O_2]$ catalyst, we were unable to observe any Mo–H bonds by using ^1H NMR spectroscopy. However, reaction of $[MoCl_2O_2]$ with $MePh_2SiH$, in the absence of aldehydes or ketones, formed the Mo^V complex $[\{MoCl_2O(OSiPh_2Me)\}_2]$. Most plausibly, this diamagnetic product results from the association of two paramagnetic species of composition $[MoCl_2O(OSiPh_2Me)]$ that would arise if one H atom were lost by homolytic cleavage of the Mo–H bond formed by means of [2+2] addition of Si–H to one of the two Mo=O bonds, as depicted in Scheme 4.

This observation suggested the possibility of having a radical mechanism operating in the hydrosilylation reaction catalyzed by $[MoCl_2O_2]$. Accordingly, the reaction is effectively

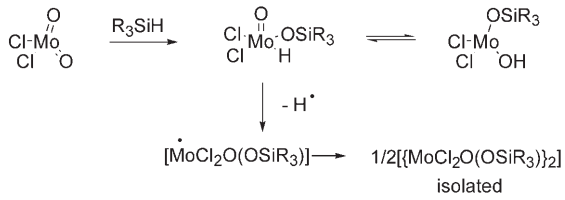

Scheme 4.

inhibited or strongly retarded upon addition of radical scavengers.[12]

We are unaware of any studies on the influence of radical scavengers in Re–oxo-catalyzed hydrosilylations and this kind of mechanism has not been addressed in the computational studies available at this time. However, the work of Mayer and Cook provided irrefutable proof of the formation of radicals in the C–H activation reactions of $[CrCl_2O_2]$.[18]

The facts described above suggest that this new type of hydrosilylation catalysis may become synthetically useful but that its intimate mechanism may present subtle differences depending on the actual type of metal–oxo core in the catalyst. In this regard, we should have in mind the classical study by Rappé and Goddard in which the fundamentals for understanding the reactivity differences of M=O and M(=O)$_2$ species towards C–H and H–H and other bonds were first laid out on the basis of molecular orbital analysis;[19] for a computational update of parts of this article see reference [20].

In the present work, we report the results of our DFT studies on the hydrosilylation of acetaldehyde catalyzed by the very active $[MoCl_2O_2]$, and we emphasize the different mechanistic possibilities of Si–H activation and the subsequent hydrosilylation activity.

Results and Discussion

Both of the dioxo complexes $[MoCl_2O_2]$ and $[ReIO_2(PR_3)_2]$ are active in the reductive chemistry described above. However, they differ in several important ways. For instance, whereas the oxidation of Re^V remains a possibility, the same is not true of Mo^{VI}, which definitely precludes oxidative addition of the Si–H bond to the metal center. On the other hand, these Re^V catalysts are formally 16-electron species, but $[MoCl_2O_2]$ has a formal 12-electron count rendering it much more unsaturated, even if π donation from the ligands is taken into account.

In the following discussion, we start by describing the Si–H activation step, and then move to the reduction of the CO-containing substrate. In an earlier computational study, Lin and co-workers[17] were unable to locate a transition state for the metathesis mechanism proposed by Abu-Omar and co-workers;[11] as a result, we did not consider this possibility. Because the Mo^{VI} complex is so electron deficient, chlorine loss is an unlikely possibility, and dissociative pathways were not taken into account. In fact, chloride dissociation from $[MoCl_2O_2]$ to give cationic species is not a common reaction pathway in the interaction of the compound with a wide variety of ligands, which usually add to the Mo center to fill the octahedral coordination sphere.

Si–H activation: Three different possibilities were considered for the activation of the Si–H bond in SiH_4: the [2+2] and [3+2] addition across one of the M=O bonds, and the [2+2] heterolytic cleavage, which gave rise to O–H and Mo–Si bonds. The starting products, $[MoCl_2O_2]$ and SiH_4, the transition states, and the final intermediates are shown in Figure 1.

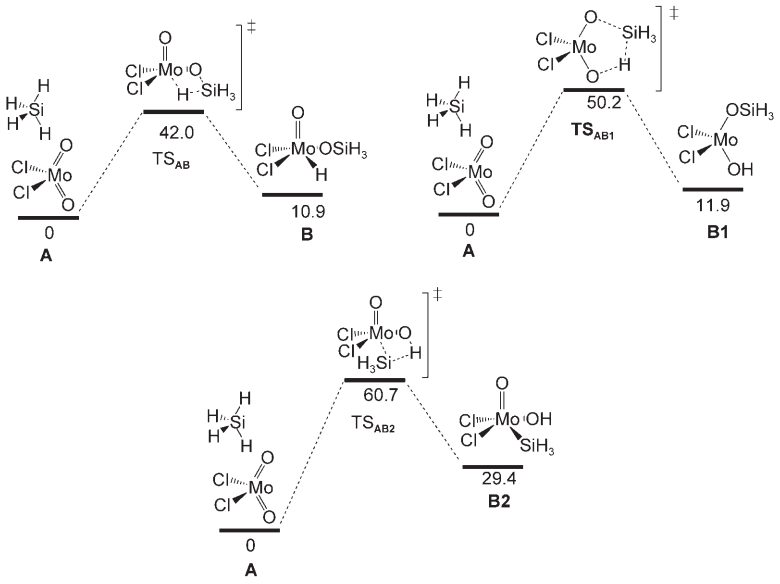

Figure 1. Three pathways for Si–H addition to $[MoCl_2O_2]$: [2+2] addition to Mo=O (top, left), [3+2] addition to Mo=O (top, right), [2+2] heterolytic addition to Mo=O (bottom); free energies are given in kcal mol^{-1}.

These reactions are endergonic and only slightly endothermic. In all cases, the most favorable situation is, however, the [2+2] Si–H addition to Mo=O. Details of the geometries of the intermediates and transition states are shown in Figure 2.

The [2+2] additions give rise to five-coordinate complexes (**B** and **B2**) displaying distorted-square-pyramidal geometries, whereas after the [3+2] addition the complex remains tetrahedral, though severely distorted. The widest Cl-Mo-Cl angle in **B1** is 142°. The large stability of intermediate **B** can

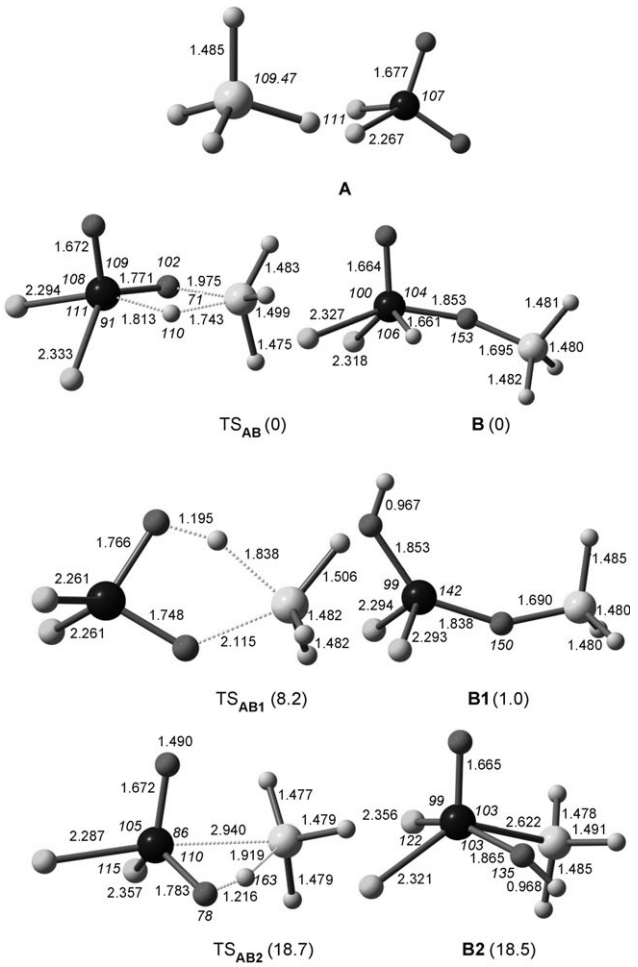

Figure 2. Optimized geometries of reagents, intermediates, and transition states, and distances [Å], angles ([°], italics), and relative free energies [kcal mol^{-1}]. The angles shown are of Cl_{ax}-Mo-X.

be assigned to the strong Mo–H bond. Although the difference is too small to be very relevant, the Mo=O bond in hydride complex **B** is shorter (1.664 Å) than it was in the initial complex **A** (1.677 Å), a trend also observed in the related chemistry of Re^{V} and considered a hallmark of the so-called oxygen spectator effect.[18,20]

Although the stabilities of products **B** and **B1** are not very different, the energy differences between the transition states are more significant, definitely favoring the hydride-mediated pathway involving a [2+2] addition. The unfavorable geometry of approach between the two reagents via TS$_{AB2}$ probably causes its high energy, whereas the steric hindrance of product **B2** may increase its energy relative to that of **B** and **B1**.

The above-calculated barriers were obtained in the gas phase. We also computed the activation barriers for the preferred [2+2] addition yielding intermediate **B** by modeling the acetonitrile solvent by a continuum model (see the Computational Details) and using $SiMe_3H$ and methane as substrates. These values are given in Table 1 and compared with those of other related studies.

Table 1. Free energies of acetonitrile solution (in parenthesis) [kcal mol^{-1}] and gas phase for the [2+2] addition of SiH_4, $SiMe_3H$, and methane to several Mo catalysts.

	A	TS$_{AB}$	B	Catalyst
SiH_4	0.0	42.0 (41.5)	10.9 (9.8)	$[MoCl_2O_2]$
$SiMe_3H$	0.0	37.9 (36.6)	3.8 (3.5)	$[MoCl_2O_2]$
CH_4	0.0	103.0	48.0	$[MoCl_2O_2]$
CH_4[a]	0.0	43.7	−21.5	$[MoO_3]$
CH_4[a]	0.0	58.6	−9.4	$[MoO_2]$
CH_4[a]	0.0	54.5	0.0	[MoO]
CH_4[b]	0.0	112.9	62.8	$[Mo_3O_9]$

[a] Ref. [21]. [b] Ref. [22].

The calculated gas-phase barrier decreases significantly when going from SiH_4 to $SiMe_3H$, and the most striking feature is the increased stability of intermediate **B** when $SiMe_3H$ is used, which makes the reaction less endergonic. The inclusion of solvent effects helps to lower the barrier even further, but this effect is much smaller than the previous one. We did not perform the same calculations for the other pathways, but for the one leading to **B1**, the effects should be similar. On the other hand, the formation of **B2** should be even more difficult if $HSiMe_3$ is used instead of SiH_4. We also tested the possibility of C–H bond activation by the $[MoCl_2O_2]$ complex, but as can be seen from the gas-phase free energies, the process has a very high barrier (103 kcal mol^{-1}) and product **B** is not stable. Notice that one of the analogous studies reported in the literature refers to a similar barrier (112.9 kcal mol^{-1}), though the others are surprisingly low.

Although it seems straightforward that **B** is the most favored intermediate, we also studied the conversion of **B** into **B1**, a process involving a 1,2-hydrogen migration from oxygen to molybdenum. Surprisingly, the computed barrier is 32.2 kcal mol^{-1}, which is lower than any of the calculated barriers for Si–H activation. The pathway is shown in Figure 3.

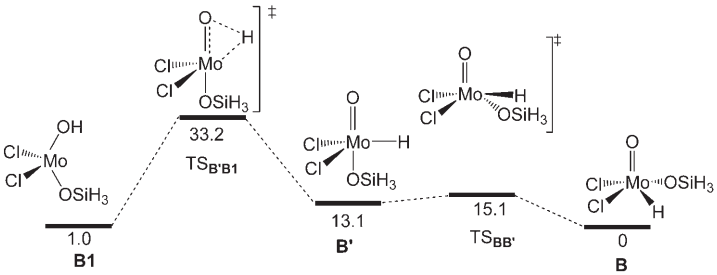

Figure 3. Free-energy profile [kcal mol^{-1}] for the conversion of $[MoCl_2(HO)(OSiH_3)]$ (**B1**) to $[MoCl_2(H)(O)(OSiH_3)]$ (**B**).

The direct product of the insertion is a trigonal-bipyramidal hydride complex (**B′**), which easily isomerizes into the thermodynamically preferred square-pyramidal form (**B**). This isomerization requires much less energy than that in the analogous Re system,[17] not excluding that an equilibri-

um between **B** and **B1** is present in the molybdenum system.

Some authors claimed that intermediates in C–H activation promoted by Mo derivatives could originate from hydrogen abstraction from the methylating agent, forming a methyl radical and a hydroxide molecule that can then recombine.[21],[22] We did not explore these pathways, because they do not seem to be relevant in the Si–H activation with $[MoCl_2O_2]$.

Aldehyde reduction: Assuming that complex **B**, $[MoCl_2H(O)(OSiH_3)]$, is the preferred intermediate, the next step involves the reduction of the carbonyl group of the aldehyde. Therefore, the aldehyde must approach complex **B**, forming a weak Mo···O bond. This is an exothermic process ($-9.5\,kcal\,mol^{-1}$), though slightly endergonic ($2.6\,kcal\,mol^{-1}$) owing to the entropy effect, and we did not look for the transition state. Two alternative pathways can take place at this stage: either a concerted mechanism, allowing simultaneous formation of the C–H and Si–O bonds in one step, or a stepwise classical reduction, in which the H atom migrates to the carbonyl carbon atom to yield an alkoxide, the silyl group migrates to the alkoxide, and the silyl ether results. These pathways are represented in Figure 4.

In the concerted mechanism, the aldehyde adduct **C** rotates, so that the C–H and the Si–O bond are formed in one step (TS_{CD}); their lengths in the transition state are 1.491 and 2.018 Å, respectively (Figure 5).

The Mo–O bond is on its way to becoming a Mo=O bond. The product formed is an adduct of the final silyl ether and the initial catalyst. This is a very efficient way of obtaining the product, with an activation barrier of about $26\,kcal\,mol^{-1}$.

In the alternative path, only the C–H bond is formed in the first step, which corresponds to the overall barrier ($\approx 24\,kcal\,mol^{-1}$) and it is rather long in TS_{CE} (1.546 Å). In the next step, the SiH_3 group migrates to the alkoxide (TS_{EA}) in a downhill process. In this final transition state, one Mo–O bond is elongating in order to break (2.094 Å), while the other one is strengthening (1.786 Å). Interestingly, the barrier for this more-complicated pathway is very similar to the concerted one. On the other hand, Lin and co-workers[17] found in their study on Re^{V} that the classical reduction was greatly favored relative to the concerted reduction (≈ 7 to $\approx 33\,kcal\,mol^{-1}$), thus supporting a clear mechanistic distinction that cannot be made in the present case.

In fact, for this molybdenum catalyst the barriers are so similar that we cannot decide on a given pathway. The detection of an alkoxide complex might indicate a preference

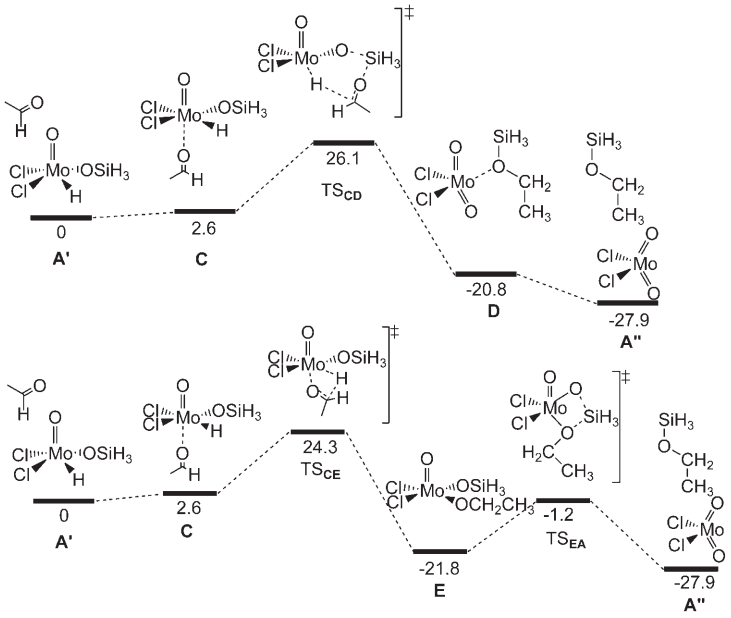

Figure 4. Free energy profile [$kcal\,mol^{-1}$] for the concerted reduction of aldehyde by $[MoCl_2(H)(O)(OSiH_3)]$ (top), and classical reduction followed by silyl migration (bottom).

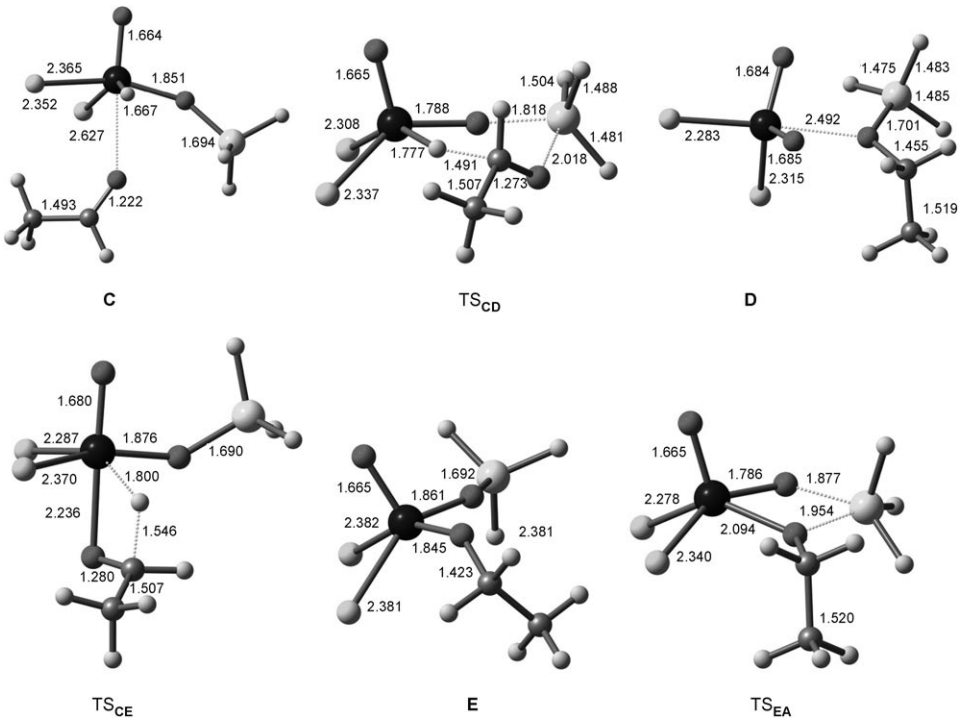

Figure 5. Optimized geometries of reagents, intermediates, and transition states, and distances [Å], for aldehyde reduction.

for the stepwise reduction. Its absence, however, does not prove anything.

Radical mechanism: As mentioned above, our experimental results showed that radical scavengers unequivocally inhibit the reaction, which suggests that a radical mechanism might play a role.[12] The treatment of the catalyst with the silylating agent without further addition of substrate led to the formation of a complex assigned as $[\{MoCl_2(O)(OSiR_3)\}_2]$ and a hydrogen radical whose fate was not established, which gave support to the same idea.

Despite the difficulties of performing calculations involving radicals, we tried to address the problem. All the calculations involving radical species had to consider the presence of solvent (acetonitrile, PCM model; see the Computational Details) and only intermediates were taken into account. This means that we could only consider the changes in free energy for the bond-breaking reactions (no transition states were located). These results give an estimation of the energy required to break a bond. The relative free energies in solution for the species involved in the radical mechanism are depicted in Figure 6.

We first considered the homolytic cleavage of complex **B** with loss of the hydrogen radical. The computed energy for the Mo–H homolytic bond splitting is about 27 kcal mol^{-1}. The alternative hypothesis of heterolytic bond splitting, yielding H^- and a metal cation, involves a much higher energy ($\approx$88 kcal mol^{-1}). This suggests that **B** is a very poor hydride donor, in agreement with the low hydricity of the $[ReH(hoz)_2(O)]^+$ complex, a species studied in relation to the $[Re(hoz)_2O]^+$ catalyst.[11]

Assuming that hydrogen radicals are formed, they could add to the aldehyde (exergonic process) forming an alkoxyl radical, which can combine with $[MoCl_2(O)(SiH_3)]^\bullet$ leading to complex **E** in a very exergonic process ($\approx$30 kcal mol^{-1}). This is the same intermediate we met in the classical reduction pathway and the remaining steps in Figure 6 were also discussed above (Figure 5). The singly occupied molecular orbitals (SOMOs) of $[MoCl_2(O)(SiH_3)]^\bullet$ and $[CH_3CH_2O]^\bullet$ as well as their spin densities are represented in Figure 7. Whereas **B** has a d^0 configuration, the radical **B**$^\bullet$ has a d^1 configuration, and the SOMO is a metal-centered orbital,

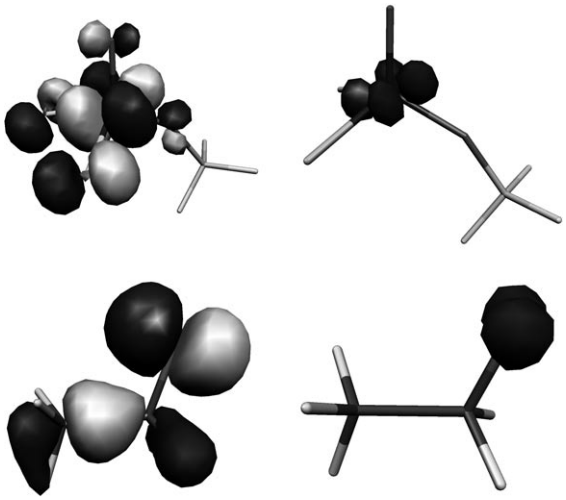

Figure 7. Representation of the SOMO (left) and spin densities (right) of radicals $[MoCl_2(O)(SiH_3)]^\bullet$ (**B**$^\bullet$) (top) and $[CH_3CH_2O]^\bullet$ (bottom).

with the spin density mainly located on the metal. The spin density of the alkoxyl radical is concentrated on the oxygen atom, reflecting the nature of the SOMO, which has a large coefficient on the oxygen atom. The recombination of these two radicals is likely to form a Mo–O bond, as proposed in the radical mechanism.

Substrate and solvent effects in the aldehyde reduction: The previous results did not suggest a clear pathway for the aldehyde reduction, as comparable barriers were determined, so the effect of the nature of the silylating agent and the role of solvent were examined in more detail. Table 2 presents the relative energies in the gas phase and in acetonitrile for the species involved in the three mechanisms considered in this study using SiH_4 and $HSiMe_3$ as silylating agents.

The introduction of solvent effects in the calculation when using SiH_4 causes the increase of the energies of all transition states. This increase is more pronounced for TS_{CD}, and makes the classical and radical mechanisms slightly preferred over the concerted one. The concerted mechanism becomes definitely noncompetitive, and can be discarded when the more realistic $HSiMe_3$ is used in the calculation in acetonitrile. TS_{CE} is not affected, whereas the energy of TS_{CD} in-

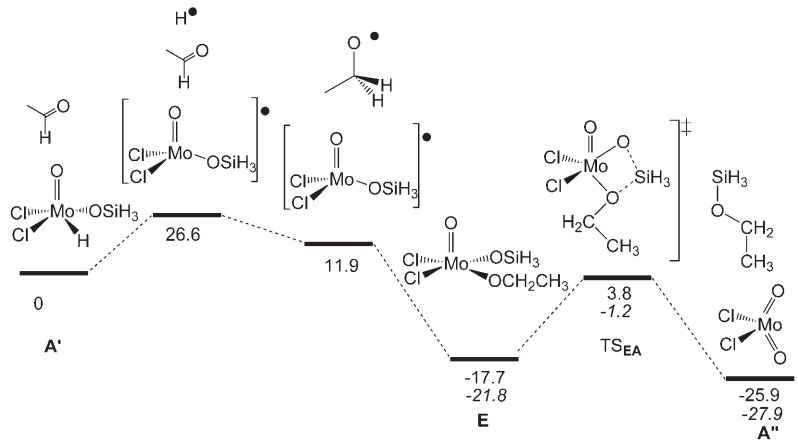

Figure 6. Free-energy profile [kcal mol^{-1}] for the loss of hydrogen radicals from complex **B** and the evolution toward the silyl ether and the regenerated catalyst in acetonitrile and in the gas phase (italics).

Table 2. Free energies of acetonitrile solution (in parenthesis) [kcal mol^{-1}] and gas phase for the species involved in the three mechanisms for aldehyde reduction using SiH_4 and $HSiMe_3$ as the silylating agent.

	SiH_4		$HSiMe_3$	
	gas phase	NCMe	gas phase	NCMe
A′	0		0	
classical				
TS_{CE}	24.3	26.1	25.9	26.2
E	−21.8	−17.7	−20.4	−17.5
TS_{EA}	−1.2	3.8	11.5	13.4
A″	−27.9	−25.9	−28.4	−22.7
concerted				
TS_{CD}	26.1	29.6	35.7	40.1
A″	−27.9	−25.9	−28.4	−22.7
radical				
B$^{\bullet}$ + H$^{\bullet}$ + CH_3CHO	–	26.6	–	29.7
B$^{\bullet}$ + $[CH_3CH_2O]^{\bullet}$	–	11.9	–	15.0

creases a lot. The energy of the homolytic splitting of the Mo−H bond also increases slightly.

The radical and classical mechanisms have similar barriers, the latter one slightly lower by 3.5 kcal mol^{-1}, which is not sufficient to provide a clear distinction between these two.

Conclusion

From the above calculations, the initial step of Si−H activation by $[MoCl_2O_2]$ is assumed to form a hydride species, $[MoCl_2H(O)(OSiR_3)]$ (**B**), as this has the lowest activation energy (42.0 kcal mol^{-1}, Figure 1). However, the participation and concurrent formation of **B1** in the reaction, which corresponds to the [3+2] addition of Si−H to $[MoCl_2O_2]$, cannot be entirely ruled out because its interconversion to **B** has lower activation energy (33.2 kcal mol^{-1}, Figure 3). Nevertheless, the intermediacy of **B** is most likely because it best explains the experimental formation of $[\{MoCl_2(O)(OSiR_3)\}_2]$, which takes place in the absence of aldehydes or ketones.

On going from hydride **B** to the final hydrosilylation reaction product, all three possibilities checked in our calculations with SiH_4 (concerted addition, classical hydride migration, and radical reaction) lead to very similar gas-phase activation energies of approximately 26 kcal mol^{-1}. However, if we consider solvent effects (NCMe) and the silylating agent is $HSiMe_3$, the concerted mechanism can be discarded, leaving the radical and classical mechanisms.

This leaves us short of being able to assign a clear mechanistic pathway for the hydrosilylation reaction under $[MoCl_2O_2]$ catalysis. In comparison, in the $[ReI(O)_2(PR_3)_2]$ system, after a first dissociation of a phoshane group, the classical reduction is significantly favored over the concerted one, but a radical alternative has not been considered yet.

In the particular system addressed, $[MoCl_2O_2]$/NCMe, the radical path is probably the most likely if the experimental data is considered. However, small changes in the system, particularly in the solvent, may play a major role and favor one of the other two alternatives. The fact that the reaction is faster in NCMe, a solvent known to assist radical processes, may be already a manifestation of such subtle differences.

Clearly, kinetic and other mechanistic studies are still necessary to probe the mechanism of this rather active catalytic system.

Computational Methods

All calculations were performed by using the Gaussian03 software package.[23] The B3LYP hybrid functional was used in all calculations. This functional includes a mixture of Hartree–Fock[24] exchange with DFT[25] exchange-correlation, given by Becke's three-parameter functional[26] with the Lee, Yang, and Parr correlation functional, which includes both local and nonlocal terms.[27,28] The geometries were optimized without any symmetry constrains by using the standard LanL2DZ basis set with the associated ECP[29] augmented with a f-polarization function (exponent 1.043) for Mo.[30] A standard 6-31G(d,p) basis set[31] was used for the other elements. Frequency calculations were performed in all species at this level of theory to confirm the nature of the stationary points. The transition-state structures, which yielded one imaginary frequency, were relaxed following the vibrational mode to confirm the connecting reagents. The reported gas-phase Gibbs free energies were also obtained at this level of theory. The Gibbs free energies in solution were obtained by performing self-consistent reaction field (SCRF) calculations using the polarizable continuum model (PCM) and the universal force field (UFF)[32] to define the atomic radii of the atoms on the gas-phase-optimized geometries.

The silylating agents were modeled by SiH_4 and $SiMe_3H$. The substrate considered was acetaldehyde.

Acknowledgement

M.J.C. and P.J.C. thank the FCT for grant POCI/QUIM/58925/2004/, and P.J.C. acknowledges the FCT for grant SFRH/BD/10535/2002.

[1] M. B. O'Donoghue, R. R. Schrock, A. M. LaPointe, W. Davis, *Organometallics* **1996**, *15*, 1334–1336.
[2] W. A. Herrmann, *Angew. Chem.* **1988**, *100*, 1269–1286; *Angew. Chem. Int. Ed. Engl.* **1988**, *27*, 1297–1313.
[3] C. C. Romão, F. E. Kühn, W. A. Herrmann, *Chem. Rev.* **1997**, *97*, 3197–3246, and references therein.
[4] a) J. H. Espenson, M. M. Abu-Omar, *Adv. Chem. Ser.* **1997**, *253*, 99–134; b) G. S. Owens, J. Aries, M. M. Abu-Omar, *Catal. Today* **2000**, *55*, 317–363.
[5] W. R. Thiel, *Angew. Chem.* **2003**, *115*, 5548–5550; *Angew. Chem. Int. Ed.* **2003**, *42*, 5390–5392.
[6] J. J. Kennedy-Smith, K. A. Nolin, H. P. Gunterman, F. D. Toste, *J. Am. Chem. Soc.* **2003**, *125*, 4056–4057.
[7] a) I. Ojima in *The Chemistry of Organosilicon Compounds* (Eds.: S. Patai, Z. Rappoport), Wiley, New York, **1989**, p. 1479; b) I. Ojima, Z. Li, J. Zhu in *The Chemistry of Organosilicon Compounds, Vol. 2* (Eds.: Z. Rappoport, Y. Apeloig), Wiley, New York, **1998**, p. 1687.
[8] a) M. J. Romão, R. Huber, *Structure and Bonding, Vol. 90*, Springer, Heidelberg, **1998**, p. 69–96; b) M. J. Romão, J. J. G. Moura, J. Knäblein, R. Huber, *Prog. Biophys. Mol. Biol.* **1997**, *68*, 121–144.
[9] A. C. Fernandes, R. Fernandes, C. C. Romão, B. Royo, *Chem. Commun.* **2005**, 213–214.
[10] B. Royo, C. C. Romão, *J. Mol. Catal. A* **2005**, *236*, 107–112.
[11] E. A. Ison, E. R. Trivedi, R. A. Corbin, M. M. Abu-Omar, *J. Am. Chem. Soc.* **2005**, *127*, 15374–15375.

[12] P. M. Reis, C. C. Romão, B. Royo, *Dalton Trans.* **2006**, 1842–1846.
[13] K. A. Nolin, R. W. Ahn, F. D. Toste, *J. Am. Chem. Soc.* **2005**, *127*, 12462–12463.
[14] A. C. Fernandes, C. C. Romão, *Tetrahedron Lett.* **2005**, *46*, 8881–8883.
[15] A. C. Fernandes, C. C. Romão, *J. Mol. Catal. A* **2006**, *253*, 96–98.
[16] A. C. Fernandes, C. C. Romão, *Tetrahedron* **2006**, *62*, 9650–9654.
[17] L. W. Chung, H. G. Lee, Z. Lin, Y. Wu, *J. Org. Chem.* **2006**, *71*, 6000–6009.
[18] G. K. Cook, J. M. Mayer, *J. Am. Chem. Soc.* **1994**, *116*, 1855–1868.
[19] A. K. Rappé, W. A. Goddard, *J. Am. Chem. Soc.* **1982**, *104*, 3287–3294.
[20] P. E. M. Siegbahn, *J. Phys. Chem.* **1993**, *97*, 9096–9102.
[21] X. Xu, F. Faglioni, W. A. Goddard, III, *J. Phys. Chem. A* **2002**, *106*, 7171.
[22] G. Fu, X. Xu, X. Lu, H. Wan, *J. Am. Chem. Soc.* **2005**, *127*, 3989–3996.
[23] Gaussian 03, Revision B.04, M. J. Frisch, G. W. Trucks, H. B. Schlegel, G. E. Scuseria, M. A. Robb, J. R. Cheeseman, J. A. Montgomery, Jr., T. Vreven, K. N. Kudin, J. C. Burant, J. M. Millam, S. S. Iyengar, J. Tomasi, V. Barone, B. Mennucci, M. Cossi, G. Scalmani, N. Rega, G. A. Petersson, H. Nakatsuji, M. Hada, M. Ehara, K. Toyota, R. Fukuda, J. Hasegawa, M. Ishida, T. Nakajima, Y. Honda, O. Kitao, H. Nakai, M. Klene, X. Li, J. E. Knox, H. P. Hratchian, J. B. Cross, V. Bakken, C. Adamo, J. Jaramillo, R. Gomperts, R. E. Stratmann, O. Yazyev, A. J. Austin, R. Cammi, C. Pomelli, J. W. Ochterski, P. Y. Ayala, K. Morokuma, G. A. Voth, P. Salvador, J. J. Dannenberg, V. G. Zakrzewski, S. Dapprich, A. D. Daniels, M. C. Strain, O. Farkas, D. K. Malick, A. D. Rabuck, K. Raghavachari, J. B. Foresman, J. V. Ortiz, Q. Cui, A. G. Baboul, S. Clifford, J. Cioslowski, B. B. Stefanov, G. Liu, A. Liashenko, P. Piskorz, I. Komaromi, R. L. Martin, D. J. Fox, T. Keith, M. A. Al-Laham, C. Y. Peng, A. Nanayakkara, M. Challacombe, P. M. W. Gill, B. Johnson, W. Chen, M. W. Wong, C. Gonzalez, J. A. Pople, Gaussian, Inc., Wallingford CT, **2004**.
[24] W. J. Hehre, L. Radom, P. von R. Schleyer, J. A. Pople, *Ab Initio Molecular Orbital Theory*, Wiley, New York, **1986**.
[25] R. G. Parr, W. Yang, *Density Functional Theory of Atoms and Molecules*, Oxford University Press, New York, **1989**.
[26] A. D. Becke, *J. Chem. Phys.* **1993**, *98*, 5648.
[27] B. Miehlich, A. Savin, H. Stoll, H. Preuss, *Chem. Phys. Lett.* **1989**, *157*, 200.
[28] C. Lee, W. Yang, R. G. Parr, *Phys. Rev. B* **1988**, *37*, 785.
[29] a) T. H. Dunning, Jr., P. J. Hay, in *Modern Theoretical Chemistry, Vol. 3* (Ed.: H. F. Schaefer, III), Plenum, New York, **1976**, p. 1; b) P. J. Hay, W. R. Wadt, *J. Chem. Phys.* **1985**, *82*, 270; c) W. R. Wadt, P. J. Hay, *J. Chem. Phys.* **1985**, *82*, 284; d) P. J. Hay, W. R. Wadt, *J. Chem. Phys.* **1985**, *82*, 2299.
[30] A. W. Ehlers, M. Böhme, S. Dapprich, A. Gobbi, A. Höllwarth, V. Jonas, K. F. Köhler, R. Stegmann, A. Veldkamp, G. Frenking, *Chem. Phys. Lett.* **1993**, *208*, 111.
[31] a) R. Ditchfield, W. J. Hehre, J. A. Pople, *J. Chem. Phys.* **1971**, *54*, 724; b) W. J. Hehre, R. Ditchfield, J. A. Pople, *J. Chem. Phys.* **1972**, *56*, 2257; c) P. C. Hariharan, J. A. Pople, *Mol. Phys.* **1974**, *27*, 209; d) M. S. Gordon, *Chem. Phys. Lett.* **1980**, *76*, 163; e) P. C. Hariharan, J. A. Pople, *Theor. Chim. Acta* **1973**, *28*, 213.
[32] A. K. Rappé, C. J. Kasewit, K. S. Colwell, W. A. Goddard, III, W. M. Skiff, *J. Am. Chem. Soc.* **1992**, *114*, 10024.

Received: November 28, 2006
Published online: March 1, 2007

